JOURNAL OF MATERIALS SCIENCE 21 (1986) 2565–2570

The effect of silicon on the eutectic grain size of gravity cast Zn–12% Al

S. A. THOMPSON, P. NIESSEN
Department of Mechanical Engineering, University of Waterloo, Waterloo, Ontario N2L 3G1, Canada

For gravity castings made from Zn–12% Al alloys wide variations of impact strength have been observed that could not be explained in terms of casting soundness. Previous unpublished research isolated trace impurities of silicon as the cause of a large increase in eutectic grain size and subsequent decrease in impact strength. In the present study the effect of silicon on the as-cast eutectic grain size and impact strength of Zn–12Al is confirmed. Thermal analysis and interface equilibration experiments indicate that silicon impedes nucleation of the eutectic β phase. Finding that the presence of silicon lowers the primary α'/eutectic liquid interfacial energy, it is concluded that silicon, rejected by the pro-eutectic α' phase during primary solidification, poisons the interface causing the difficulty with the nucleation of eutectic β on the primary α' surface leading to the increase in eutectic grain size.

1. Introduction

Zinc–aluminium alloys are used extensively in die-casting applications. The attractiveness of these zinc alloys is due to their excellent castability, good mechanical properties and machinability. The aluminium content of these die-cast alloys is typically slightly below, but very close to the eutectic composition at 5% Al (wt %). However since the early 60s [1], hypereutectic Zn–Al alloys containing between 8 and 27% Al have steadily gained popularity as gravity cast foundry alloys. The 12% aluminium alloy is the most commonly used for foundry work because of its superior strength, hardness and casting versatility. This alloy has, in many cases, become an attractive alternative to cast iron, brass, bronze and aluminium-based casting alloys [2].

The aluminium-rich hypereutectic Zn–Al alloys have a structure consisting of the pro-eutectic and eutectic f c c α' phase (17.8% Al) and the eutectic h c p β phase (1% Al). On cooling from the eutectic temperature (382° C), the α' phase rejects zinc until the composition 22% Al is reached at 275° C when the α' undergoes a eutectoid reaction producing β (0.6% Al) and the aluminium-rich α (31.6% Al).

One detrimental aspect of the Zn–12% Al alloys, which also contain small amounts of copper and magnesium, and are commercially known as ILZRO 12, Korloy 2570 or ZA 12, is their rather unpredictable impact strength ranging between 6 and 18 ft lb (8 to 24 J) on unnotched Charpy specimens at room temperature [3].

In previous unpublished research, Elshiek [4] found even larger variations in impact strength. He also showed that these large variations are not due to casting defects. Rather, he isolated trace impurities of silicon as the cause of a large increase in eutectic grain size which leads to a lower impact strength. The effect of silicon on impact strength is shown in Fig. 1. The grains, which predominantly fail by a cleavage mechanism, are defined by the β-phase of the eutectic. The fracture front follows the basal plane of the β matrix and ruptures or pulls out primary α' in its path. Since grain boundaries hinder cleavage propagation, a smaller grain size results in a higher impact strength. Elshiek cast high purity Zn–12% Al in a heated (200° C) steel mould and found the average grain size to be 90 μm. An alloy of the same composition but containing 0.04% Si had an average grain size of 400 μm when cast under the same conditions.

Elshiek argued that silicon exerted a poisoning influence on the α'/β interface. Silicon, it was believed, obliterated the epitaxial relationship of the pure alloy thereby affecting growth and nucleation. Phase orientations in the pure Zn–12% Al are confined by epitaxial constraints, therefore growth in specified directions may be restricted and less able to respond to the direction of heat flow. In this case, renucleation of the eutectic must take place more frequently to satisfy undercooling. In the presence of silicon, however, the epitaxial constraint is relaxed, thus once nucleated, a eutectic grain will grow over longer distances with less hindrance than with the case of the pure alloy.

In recent work with hypereutectic Zn–Al cast alloys, we observed effects that were not in accord with the above hypothesis. It was therefore decided to confirm the influence of silicon on the cast structure of Zn–Al alloys and further explore how silicon exerts its influence.

2. Experimental procedure and results

2.1. Effect of silicon on the grain size of Zn–12% Al

Samples of high purity Zn–12% Al and the silicon-bearing Zn–12% Al–0.1% Si were prepared from special high grade zinc and high purity aluminium. The silicon was introduced by means of an

0022–2461/86 $03.00 + .12

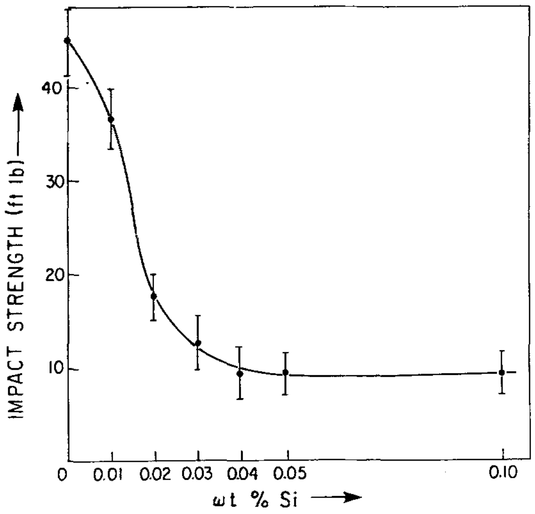

Figure 1 Effect of silicon content on the room temperature impact strength of Zn–12% Al unnotched Charpy specimens (from [4]).

aluminium–silicon master alloy. The samples were melted at 600° C and cast from 520° C into a room temperature graphite mould. The cylindrical mould was 100 mm in length with an i.d. of 15 mm. The cast samples were notched and fractured by an impact blow and the fracture surfaces examined.

The high purity alloy exhibited extremely fine fracture facets while the fracture surface of the alloy containing silicon showed very coarse cleavage facets (Fig. 2). Although impact strengths were not measured in this experiment, it should be pointed out that, in agreement with Elshiek's findings, the pure alloys were much more difficult to fracture.

The cleavage facets visible on the fracture surfaces correspond to the eutectic grains. This is shown in Fig. 3 where a section perpendicular to a fracture surface was polished and examined under polarized light to contrast the different orientations of the hcp β-phase.

A quantitative comparison of grain size was conducted for three Zn–12% Al alloys containing 0.00, 0.05, 0.10% Si. Eight samples of each alloy were cast into the cylindrical graphite mould in the previously described manner. The samples were sectioned, polished and examined under polarized light. An estimate of average grain size was obtained by counting the number of grain boundaries across the polished section and dividing by the sample width. The results are presented in the first column of Table I. Typical sections which show the difference in grain size between the pure and silicon-bearing alloy are presented in Fig. 4.

TABLE I Effect of silicon on the grain size (μm) of different Zn–Al alloys

Silicon addition (wt %)	Aluminium (wt %)		
	12	6	4
0.00 (high purity)	87	211	221
0.05	431	239	223
0.10	466	244	216

Clearly a silicon effect does exist. The addition of as little as 0.05% Si results in a considerable increase in eutectic grain size.

The question arose whether germanium, a metalloid like silicon, having complete solid solubility with silicon and otherwise exhibiting very similar chemical behaviour to that of silicon, would induce a similar effect on the as-cast grain size of Zn–12% Al.

Samples of Zn–12% Al were prepared with 0.3% germanium to ensure an atomic fraction equivalent to the usual 0.1% silicon. Later samples were prepared with 0.7% germanium to account for the greater solubility in aluminium and zinc for germanium than for silicon. In either case, cast samples of both germanium levels demonstrated the fine fracture surface typical of the high-purity alloy. Clearly germanium, unlike silicon, does not cause an increase in the as-cast eutectic grain size.

2.2. Variation of the silicon effect with changing aluminium content

The effect of silicon on the eutectic grain size of hypoeutectic (Zn–4% Al) and slightly hypereutectic (Zn–6% Al) was determined. High purity and silicon-bearing (0.05% and 0.10% Si) samples of both alloys were melted and cast in the previously described manner into the cylindrical graphite moulds. The samples were sectioned and examined under polarized light for a determination of average grain size. The results,

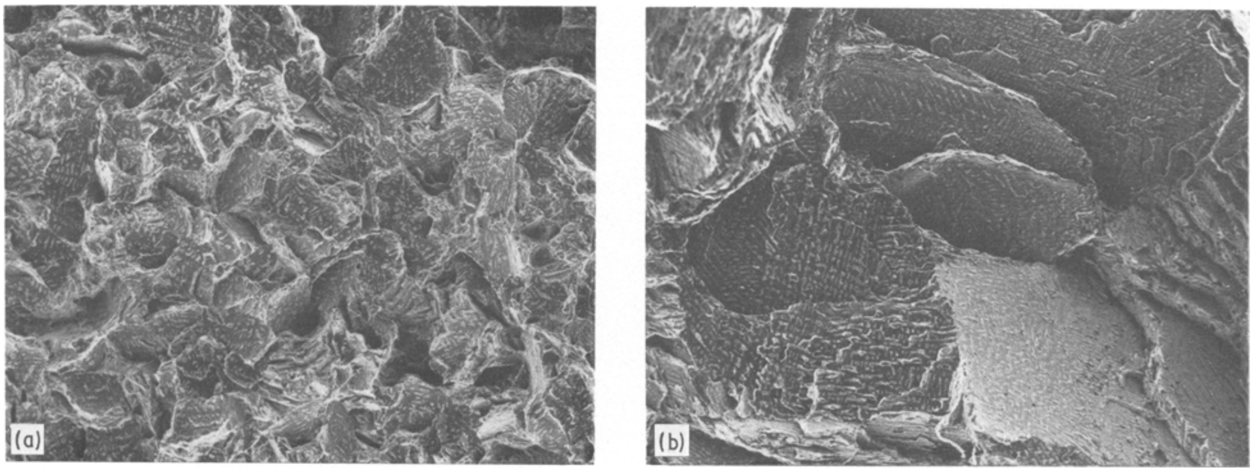

Figure 2 Scanning electron micrographs of fracture surfaces (×70) of (a) high-purity Zn–12% Al; (b) Zn–12% Al–0.1% Si.

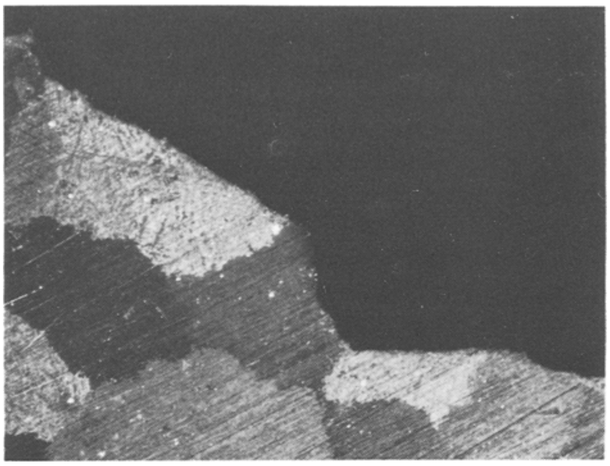

Figure 3 Section perpendicular to fracture surface showing cleaved eutectic grains as defined by the β-phase matrix. (Polarized light, × 28).

which are compared to the grain sizes previously estimated for the 12% Al alloy, are presented in Table I.

It is seen that silicon has no influence on the hypoeutectic (zinc-rich) alloys and a reduced influence on the 6% Al hypereutectic alloy. These observations suggest that silicon only affects the eutectic grain size of hypereutectic Zn–Al alloys.

2.3. Solubility of silicon in the Zn–Al system

Several experiments were undertaken to study the solubility of silicon in the various phases of the Zn–Al system. Silicon exhibits some solubility in aluminium (maximum 1.59% at 577° C) but has negligible solubility in solid zinc and very low solubility in liquid zinc below 600° C. No phase relationship data have been published on the Zn–Al–Si ternary system.

For the present work it is important to determine the solubility of silicon in the α' phase which has an aluminium fcc structure but is predominantly zinc in composition. Five alloys of the α' phase containing 0.01% to 0.05% silicon in Zn–18% Al were prepared. The molten samples were furnace cooled from 600 to 380° C and held at that temperature for 2 h. The samples were then quenched and sectioned to examine for the presence of silicon particles (silicon does not form compounds with either aluminium or zinc).

The results did not allow for an estimation of the silicon solubility in α' at the eutectic temperature because even at the lowest silicon concentration, crystals of silicon were evident in the microstructure. Therefore, it can only be stated that at 380° C the solubility of silicon in α' is below 0.01%.

Examining the as-cast Zn–12% Al microstructure, it was noticed that silicon crystals were most often found at the primary α'/eutectic interface. This is evident from the scanning electron micrograph of Fig. 5, showing a silicon crystal on an α' dendrite from the wall of a shrinkage cavity. In Fig. 5, the facets evident on the dendrite were shown by microprobe X-ray analysis to be the surface of a layer of the zinc-rich β-phase coating the α' dendrite underneath. The droplets evident on the dendrite are believed to be pure zinc condensed from the shrinkage cavity atmosphere on cooling.

The question arose whether the silicon crystals precipitated prior to the primary phase and were pushed ahead of the growing dendrites or the silicon crystals formed from the silicon rejected by the growing primary α' phase. To determine this, a Zn–12% Al–0.1% Si ingot was held slightly above the liquidus temperature at 440° C. It was believed that if silicon precipitated prior to the primary phase, the silicon particles, being of very low density, would rise to the melt surface. After 48 h the sample was allowed to solidify undisturbed. The top quarter of the frozen ingot was removed, sectioned and examined for evidence of a layer of silicon crystals. No unusual quantity of silicon was noted at or near the top. The remaining ingot was remelted, cast and fractured. The resulting coarse fracture surface clearly indicated the as-cast grain structure was still influenced by the presence of silicon.

It is therefore concluded that, despite the low solubility of silicon in the pure liquid zinc, 0.1% silicon is soluble in molten Zn–12% Al below the liquidus. It seems therefore, given the low solubility of silicon in α' and the frequent observation of silicon crystals lying across the α'/eutectic interface, that a silicon-enriched layer exists ahead of the growing primary α' phase. From this enriched layer the silicon crystals precipitated in the late stage of primary solidification.

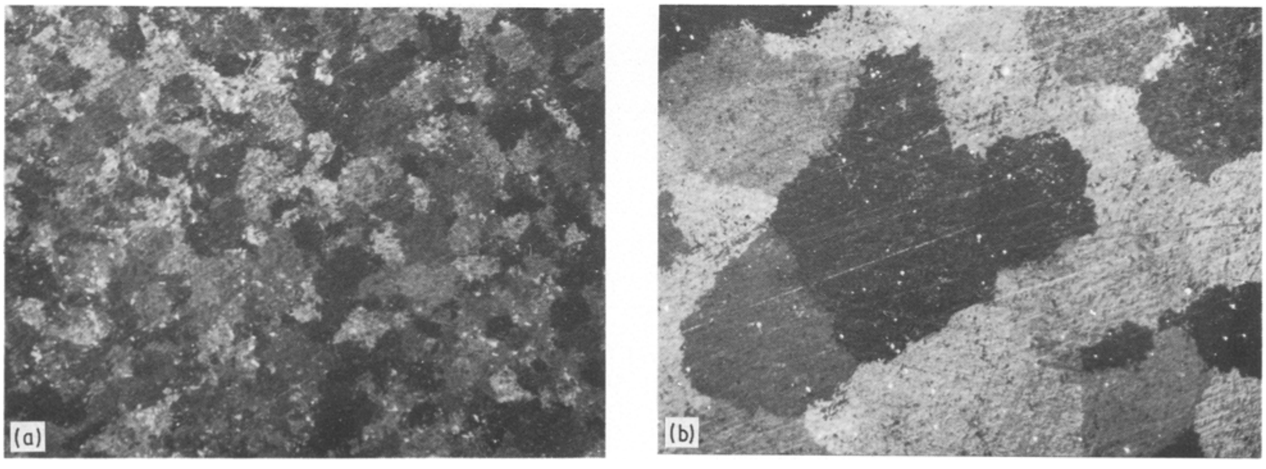

Figure 4 As-cast grain structure (polarized light, × 28). (a) High purity Zn–12% Al; (b) Zn–12% Al–0.1% Si.

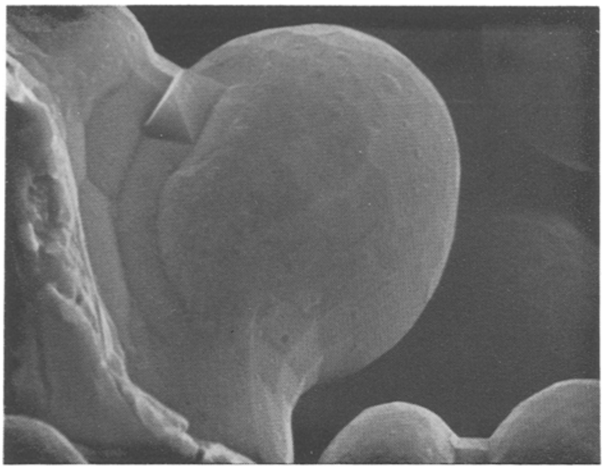

Figure 5 Scanning electron micrograph of α' dendrite with silicon crystal in Zn–12% Al–0.1% Si (×1400).

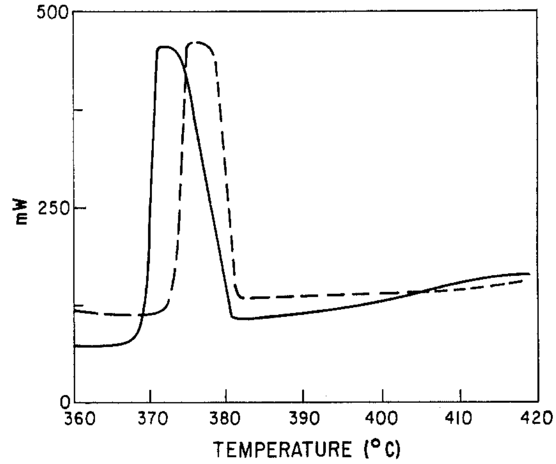

Figure 6 DSC plots: Zn–12% Al with and without silicon addition; solidified at 50° C min^{-1}. (——) Silicon alloy, (---) high purity alloy.

2.4. Thermal analysis

The nucleation of pure and silicon-bearing Zn–Al alloys was studied using differential scanning calorimetry (DSC).

Samples weighing 20 mg were cut from splat-cooled Zn–12% Al and Zn–12% Al–0.1% Si. The alloys were splat-cooled to ensure a fine distribution of the primary and eutectic phases so that the composition of the small samples was reasonably uniform. In thermal analysis, the samples were solidified at 50° C min^{-1} from 450 to 350° C and then remelted at a rate of 5° C min^{-1} from 350 to 450° C. A plot of the energy absorbed or evolved relative to a reference sample of aluminium was recorded.

The undercooling required for eutectic nucleation was estimated by subtracting the temperature for the onset of the eutectic solidification peak from the temperature of the onset of eutectic melting peak. By this method, the estimated undercooling was found to be 6.4° C for the pure alloy and 8.6° C for the silicon-bearing alloy.

A plot of the energy evolved on cooling for the silicon-bearing and high purity Zn–12% Al is presented, for a temperature range showing only the eutectic peak, in Fig. 6. It can be clearly seen that the rate of heat evolution corresponding to eutectic solidification is lower for the silicon-bearing alloy than the pure alloy. This lagging slope effect was found to be typical of the silicon-bearing alloys. Germanium, as an impurity element, was shown not to have an effect on the as-cast grain size of Zn–12% Al, nor did Zn–12% Al–0.3% Ge exhibit the lagging eutectic slope in comparison to the pure alloy when analysed using DSC. This result allows us to conclude that the slower rate of heat evolution characterizes the effect of silicon on the kinetics of eutectic solidification and not simply a modification by a ternary element of the Zn–Al phase diagram.

2.5. Equilibration experiments

The equilibration of liquid pockets in solid h c p metallic systems was employed by Miller and Chadwick [5] who reported the shape of liquid pockets adapts to preferentially expose low energy crystallographic surfaces for systems where interfacial energy is a function of orientation. In the present study, a similar technique was used to examine the relative influence of silicon on the α' interfacial energy by comparing the shape of eutectic liquid pockets and interfaces.

Samples of high purity Zn–17.6% Al and Zn–17.6% Al–0.1% Si were held for 5 days in a salt bath at 395° C. The composition of the α' phase extends to 17.8% Al. Thus a sample of marginally lower aluminium content equilibrated at a slightly higher than eutectic temperature should contain pockets of eutectic liquid in an α' matrix.

After the equilibration period, the salt bath heater was turned off and the specimens allowed to slowly cool to 365° C at which point they were removed and quenched. It was reasoned that by slow cooling, undisturbed past the eutectic temperature followed by quenching, the equilibrated interfaces would remain intact and not be obscured by the rejection of zinc from the α' phase and subsequent eutectoid transformation.

Micrographs of the equilibrated structures are presented in Fig. 7. The difference between the pure and silicon bearing alloy is striking. The α'/liquid interface of the silicon alloy is characteristically rough and irregular, the entrained liquid pockets exhibit no typical geometry to indicate an α' interfacial energy anisotropy. On the other hand, the pure alloy shows very smooth interfaces and a relative absence of internal liquid pockets. All the eutectic liquid is distributed outside the primary phase.

The microstructures of the samples prior to equilibration were examined and found to be the same. It must therefore be concluded that the difference in the equilibrated microstructures results from a difference in interfacial energies. The driving force to minimize surface energy is clearly lower in the presence of silicon.

A further experiment was conducted to determine the influence of silicon on the β/liquid interfacial energy. Samples of high purity and silicon bearing hypoeutectic Zn–2% Al were equilibrated for 5 days at 385° C. An examination of the microstructure did not reveal any difference in the morphology of the

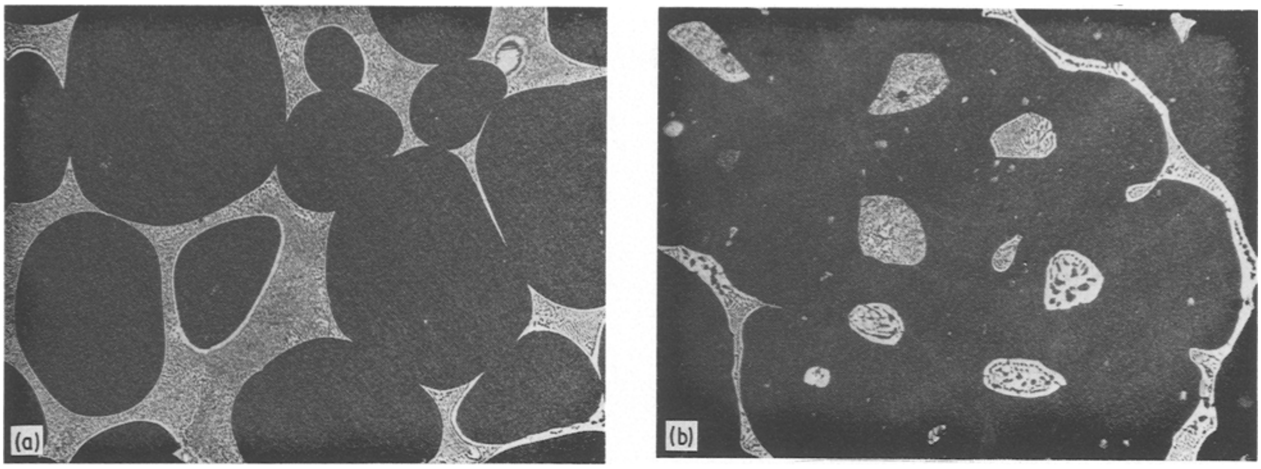

Figure 7 Microstructures equilibriated at 395° C of: (a) high-purity Zn–17.6% Al; (b) Zn–17.6% Al–0.1% Si; both at × 70.

primary β-phase between the silicon-bearing and high purity alloy. It was therefore concluded that the β/eutectic liquid interfacial energy, unlike the α'/eutectic liquid interfacial energy, is not affected by the presence of silicon.

3. Discussion of results

The pronounced effect of silicon on the as-cast eutectic grain size of the Zn–12% Al has been reaffirmed. It was found that the presence of even trace amounts of silicon (as little as 0.05%) is sufficient to cause a large increase in the eutectic grain size which is defined by the β-phase of the eutectic.

Under impact, this alloy fails by cleavage through the hcp β matrix. Since propagation of the fracture front is hindered by grain boundaries, the large grain size of the silicon-bearing alloy leads to significantly lower impact strength values. This was demonstrated by Elshiek and is confirmed in the present study. Therefore if high impact strength is required of Zn–12% Al castings, it is important to control the silicon content. Knowing from Elshiek's work that the silicon effect is well established at 0.02% (see Fig. 1), aluminium to make up a melt should contain less than 0.2% silicon. If secondary aluminium is used, great care must be taken to keep silicon alloys out of the charge.

In the present study, it was determined that germanium, a metalloid with similar chemical behaviour to silicon, has no effect on the morphology or eutectic grain size of cast Zn–12% Al. Further, the strong effect of silicon seen in the 12% Al alloy does not at all appear in hypoeutectic Zn–Al, i.e. alloys with less than 5% Al.

Because the presence of silicon has no influence on hypoeutectic alloys it can be concluded that silicon does not affect either the nucleation of the α' phase of the eutectic or the growth of the eutectic. Therefore, the formation of large grains in silicon-bearing hypereutectic alloys must be due to a more difficult nucleation of the eutectic β-phase and not the modification of growth constraints proposed by Elshiek.

The detrimental influence of silicon on eutectic nucleation in hypereutectic alloys was confirmed by thermal analysis. Using DSC, the undercooling required for eutectic nucleation was estimated by subtracting the onset temperature of eutectic solidification from the onset temperature of eutectic melting. By this method, the undercooling was found to be greater for the silicon-bearing alloy than the high purity alloy (8.64° C compared to 6.42° C). However, the effect of silicon, in this experiment was more apparent on the rate of evolution of latent heat of fusion during eutectic solidification. From Fig. 6, the eutectic solidification slope was found to be lower in the silicon-bearing alloy in comparison to the pure alloy. This is interpreted to mean the frequency of eutectic nucleation is lower in the sample containing silicon. The alternative interpretation, that the eutectic growth rate is slower in the presence of silicon, is not compatible with the observed large as-cast eutectic grains in these alloys and the absence of any morphological differences between the pure and impure alloy which would suggest different growth rates.

One may attempt to explain the role of silicon in forming large grains on the basis that the addition of a ternary element, in this case silicon, lowers the eutectic temperature [6]. However, such an explanation would not be in keeping with the results of the DSC experiments because it was found that the eutectic melting temperatures were identical for the pure and silicon-bearing alloys.

The question now stand: how does silicon influence eutectic nucleation? Does the silicon reduce the nucleation efficiency of a yet unidentified β-phase nucleant such as oxide particles, or does silicon modify the primary α' surface making it a poorer nucleation substrate? The ability of trace impurities to reduce the nucleation efficiency of an oxide was shown by Leone *et al.* [7] who examined the effect of trace impurities of lead on the grain size of Zn–Ti alloys. Obviously, at this point it would be most useful to identify the predominant β-phase nucleant.

In the present study no specific experiments were conducted to isolate the principal eutectic nucleant. However, microstructural evidence such as that presented in Fig. 8, showing eutectic lamallae radiating from an α' dendrite supports the suggestion that the primary α' phase is the principal nucleant for the β-phase of the eutectic. Accepting this, the question

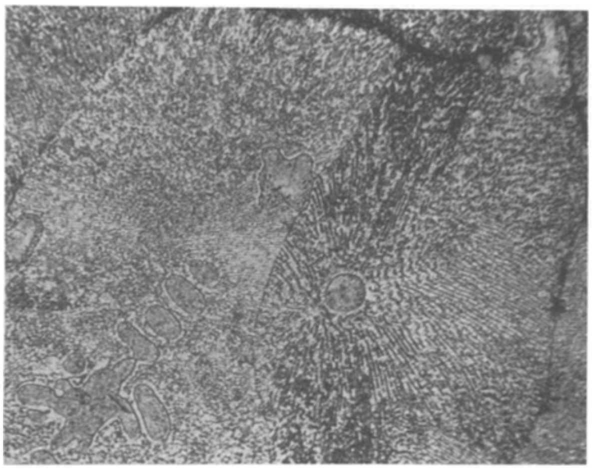

Figure 8 As-cast Zn–6% Al showing α' dendrite as the eutectic nucleant (× 175).

can be narrowed to: how does silicon reduce the efficiency of α' as the β phase nucleant?

The results of the equilibration experiments provide an answer to this question. From Fig. 7, the relative smoothness of the pure α'/liquid interface compared to the silicon-bearing alloy suggests that α'/liquid surface tension is lower in the presence of silicon. Consider now the wetting angle of a β nucleus on an α' substrate as a function of surface tensions:

$$\cos\theta = \frac{\sigma_{\alpha/L} - \sigma_{\beta/\alpha}}{\sigma_{\beta/L}} \qquad (1)$$

From Equation 1, it can be seen that a lower α'/liquid surface tension will result in a higher contact angle. The larger nucleus associated with the larger contact angle can only form at a larger undercooling. Thus in the presence of silicon the lower α'/liquid surface tension presents a greater obstacle to the nucleation of the eutectic β-phase.

The inherent assumption that the remaining surface tension terms of Equation 1 do not appreciably change with the addition of silicon is not unreasonable. In the present study, the absence of any difference between the eutectic morphology of the pure and silicon-bearing alloy suggests that the α'/β interface tension does not change. The equilibration of primary β with eutectic liquid likewise failed to reveal a difference between the structures of the pure and silicon-bearing alloy. This suggests that the β/liquid interfacial energy does not change with the addition of silicon leaving only the α'/liquid interfacial energy lowered in the presence of silicon.

It should be noted that the silicon effect demonstrated in this work was obtained when the Zn–12% Al alloy was solidified under moderate freezing rates. Under the casting parameters and mould dimensions given earlier, total solification times are of the order of 10 to 30 sec. It would be interesting to see if the silicon effect disappears at either very slow or high freezing rates. Attenuation of the silicon effect at these two extremes is to be expected if the above model for the role of silicon is true.

4. Conclusions

The present study has confirmed that the presence of trace amounts of silicon causes a large increase in the as-cast eutectic grain size and a subsequent decrease in impact strength of Zn–12% Al. From experiments conducted in this work the following conclusions are made.

1. The effect of silicon on the as-cast eutectic grain size of Zn–12% Al does not extend to hypoeutectic alloys and that germanium, unlike silicon has no influence on the eutectic grain size of Zn–12% Al.
2. In hypereutectic Zn–Al, silicon exerts its influence by impeding the nucleation of the eutectic β phase and not by assisting eutectic growth through relaxation of epitaxial growth constraints as suggested by Elshiek.
3. An enriched layer of silicon exists in the eutectic liquid ahead of the growing pro-eutectic α' phase and that the primary α' phase is most likely the nucleant for the eutectic β phase.
4. The presence of silicon at the primary α'/eutectic liquid interface lowers the interfacial energy which would increase the undercooling required for eutectic β nucleation.

Acknowledgements

Financial support for this work was provided by the Natural Sciences and Engineering Research Council of Canada. We would also like to thank the Product Research Centre of COMINCO for donation of the high purity metals used in this investigation.

References

1. E. A. ANDERSON and G. L. WERLEY, ILZRO Research Summary, Project ZM-5 (July 1962).
2. D. APELIAN, M. PALIWAL and D. C. HERRSCHAFT, *J. Metals* **33** (1981) 11.
3. S. SAKAR and A. P. BATES, Technical Report on ILZRO, Project ZM-104 (May 1967).
4. A. M. ELSHIEK, PhD thesis, University of Waterloo, Waterloo, Ontario, Canada (1975).
5. W. A. MILLER and G. A. CHADWICK, *Proc. R. Soc. Lond.* **312A** (1969) 257.
6. C. H. P. LUPIS, *Met. Trans.* **9B** (1978) 231.
7. G. L. LEONE, P. NIESSEN and H. W. KERR, *ibid.* **6B** (1975) 503.

Received 12 August
and accepted 3 October 1985